Stability of plane Couette flow of a power-law fluid past a neo-Hookean solid at arbitrary Reynolds number

D. Giribabu and V. Shankar

Citation: Physics of Fluids **29**, 074106 (2017); doi: 10.1063/1.4995295
View online: http://dx.doi.org/10.1063/1.4995295
View Table of Contents: http://aip.scitation.org/toc/phf/29/7
Published by the American Institute of Physics

Stability of plane Couette flow of a power-law fluid past a neo-Hookean solid at arbitrary Reynolds number

D. Giribabu and V. Shankar[a)]
Department of Chemical Engineering, Indian Institute of Technology, Kanpur 208016, India

(Received 14 March 2017; accepted 4 July 2017; published online 25 July 2017)

The linear stability of plane Couette flow of a power-law fluid past a deformable solid is analyzed at arbitrary Reynolds number (Re). For flow of a Newtonian fluid past a deformable solid, at high Re, there are two different modes of instability: (i) "wall modes" ($\Gamma \propto Re^{-1/3}$) and (ii) "inviscid modes" ($\Gamma \propto Re^{-1}$) where $\Gamma = \frac{V\mu_f}{GR}$ is the non-dimensional shear-rate in the fluid (V, μ_f, G, and R denote the top-plate velocity, fluid viscosity, shear modulus of the solid, and fluid thickness, respectively). In this work, we consider the power-law model for the fluid to elucidate the effect of shear-thickening/shear-thinning behaviour on the modes of instability present in the flow, especially at moderate and high Re. At high Re, our numerical results show that wall modes exhibit different scalings in Γ ($\frac{V\eta_f}{GR}$, where η_f is Newtonian-like constant viscosity) vs Re for different values of the power-law index (n), and the scaling exponents are different from that for a Newtonian fluid. This drastic modification in the scaling of wall modes is not observed in viscoelastic (modelled as upper-convected Maxwell or Oldroyd-B fluids) plane Couette flow past a deformable solid. We show that the difference in scaling exponents can be explained by postulating that the wall modes in a power-law fluid are determined by the actual viscosity corresponding to the shear rate of the laminar flow denoted by η_{app}. A non-dimensional shear rate based on this viscosity $\Gamma_{app} = \frac{V\eta_{app}}{GR}$ can be defined, and we show that the postulate $\Gamma_{app} \sim Re^{-1/3}$ (motivated by the wall-mode scaling in a Newtonian fluid) captures all the numerically observed scalings for Γ vs Re for different values of $n > 0.3$, which is found to be $\Gamma \sim Re^{\frac{-1}{2n+1}}$. Further, we numerically evaluated the wall layer thickness and this agreed with the theoretical scaling of $\delta \sim Re^{\frac{-n}{2n+1}}$. Interestingly, the theoretical and numerical prediction of wall modes is found to be valid for power-law index, $n \geq 0.3$. For $n \leq 0.3$, there is a marked departure from the wall-mode scalings, and our results show a scaling of $\Gamma \sim Re^{-1}$ corresponding to inviscid modes. The variation of the power-law index (n) can stabilise/destabilise the inviscid mode when compared with Newtonian fluid, and this result is observed only in the power-law model and is not seen in the flow of viscoelastic fluid past deformable surfaces. Thus, the present study shows that the shear-rate dependence of viscosity has a significant impact on both the qualitative and quantitative aspects of stability of non-Newtonian fluid flow past deformable surfaces. *Published by AIP Publishing.* [http://dx.doi.org/10.1063/1.4995295]

I. INTRODUCTION

In addition to polymer solutions and melts, many biological fluids such as blood, saliva, and synovial fluid are also non-Newtonian in nature. Flow of such non-Newtonian fluids past deformable solid surfaces is frequently encountered in biological flows, where it is necessary to have an understanding of laminar or turbulent nature of the flow regime. Technological applications such as microfluidic devices and *lab-on-chip* applications often also involve fluid flow past a deformable surface, especially when the devices are fabricated using elastomers.[1] Flow in such micro-scale devices occur in dimensions in the range of microns to sub-millimeters. At such small length scales, the flow tends to be laminar, and the transport is often diffusion limited resulting in poor mixing. Several strategies[2–5] (both active and passive) have been suggested to enhance mixing in microfluidic devices. These methods are associated with issues of high pressure drops, external moving parts, and difficulties in scaling down. Flow past deformable surfaces could be a potential alternative when compared with other strategies because of less moving parts and ease of fabrication.

Recent experiments of Kumaran and Bandaru[6] showed complete mixing of two streams in a turbulent flow in a channel with deformable walls at $Re \approx 226$ in a 35 μm width channel. They also showed that the time required for mixing is enhanced by several orders of magnitude when compared with laminar flow. More recent experimental work of Srinivas and Kumaran[7] showed that the addition of small amounts of polymer to the fluid decreases the critical Reynolds number in a channel flow, which is qualitatively similar to the theoretical predictions[8] for a plane Couette flow. The Reynolds number in biological flows ranges from 10^{-3} in capillaries to 6000 in arteries. Hence, it is of importance to study the stability of non-Newtonian fluid flow past deformable walls for a range of Re from low to high. For a Newtonian fluid, there are two different modes present at high Re and they are the *wall mode*

a)Author to whom correspondence should be addressed: vshankar@iitk.ac.in

instability that has a boundary layer thickness that scales as $O(Re^{-1/3})$ near the wall and the *inviscid mode* instability that has a boundary layer thickness that scales as $O(Re^{-1/2})$ near the wall. In this thin wall layer, viscous forces are dominant. Earlier work by Kumar and Shankar[9] as well as by Chokshi *et al.*[8] have focused on the role of viscoelasticity on the stability of the flow at high *Re*, but the role of the shear-rate dependence of viscosity in a non-Newtonian fluid on the stability has not been adequately addressed in the literature, especially at finite and high *Re*. In the present work, we therefore consider the stability of plane Couette flow of the non-Newtonian power-law fluid to examine the role of strain-rate dependent viscosity on the instabilities in the flow past a deformable solid at arbitrary *Re*.

We briefly recapitulate the relevant previous work on the flow of non-Newtonian fluids over rigid surfaces, followed by a review of studies on flow past (of both Newtonian and non-Newtonian fluids) deformable solid surfaces. For plane Couette flow of a Newtonian fluid at high *Re*, Romanov[10] showed that there are only *wall modes* that are stable and form boundary layers on both rigid walls. In industrial applications, we often encounter the flow of non-Newtonian fluids (polymeric melts, emulsions, and suspensions); however, not much work has been done in the literature both theoretically and experimentally. Waters[11] examined the effect of shear-thinning/shear-thickening on the stability results of stratified fluids in plane Couette flow. Khomami and co-workers[12,13] studied the interfacial stability of stratified power-law fluids in a channel and showed that shear-thinning fluid affects the stability, both for viscosity ratio less than and greater than one. Nouar *et al.*[14] studied the stratified flow of Carreau fluids with perturbation in viscosity in a channel and showed that it is possible to delay the transition. Their results differed from the previous work[15] of Chikkadi *et al.*, who considered the same problem with no perturbation in viscosity. Delaying the transition has great significance especially in the transportation of oils and polymeric solutions that reduces drag and the cost of transportation. Transient growth studies of power-law fluid in Couette flow have been carried out by Liu and Liu,[16,17] and they showed that shear-thinning has an effect on the growth of external excitations both for 2D and 3D perturbations. They also showed that the Couette flow of a power-law fluid is also linearly stable just like the Newtonian fluid but shear-thinning/shear-thickening behaviour can make eigenvalues destabilise/stabilise when compared with eigenvalues of Newtonian fluid. An explanation of their results was provided by considering an energy budget of the Orr-Sommerfeld equation, and it was shown that there are two terms, viscous stratification and perturbation in viscosity that can stabilise/destabilise the flow. In plane Couette flow, there is no viscous stratification and hence there is only perturbation in viscosity that is the destabilising force, whereas in the case of channel flow, viscous stratification stabilises the flow.[14] Liu and Liu[18] considered the pipe flow of shear-thinning fluid modelled as a Carreau fluid and studied both the response to external excitations by observing the ϵ-pseudospectra and response to initial condition. Energy growth function for azimuthal wavenumber ($m = 1$) shows the largest amplification among all non-axisymmetric cases, but the flow is still asymptotically stable.

Fluid flow past deformable surfaces has garnered much attention in the last two decades, and here, we briefly review the previous works concerning wall modes and inviscid modes. Theoretical work past a deformable solid by Kumaran[19,20] showed that there are no unstable inviscid modes in plane Couette flow and in Hagen-Poiseuille flow subjected to axisymmetric disturbances. Shankar and Kumaran[21] analyzed the stability wall modes past a deformable solid using both asymptotic (at high *Re*) and numerical methods. They found that the critical *Re* for wall modes scales as $Re \sim \Sigma^{3/4}$ in the limit $Re \gg 1$, where $\Sigma = \frac{\rho G R^2}{\eta^2}$ ($\rho, G,$ and R, η are density, shear modulus, fluid thickness, and viscosity, respectively). Chokshi *et al.*[8] performed linear stability analysis of plane Couette flow using Oldroyd-B fluid, and they showed that the addition of polymer can destabilise the flow at high *Re*, but at moderate *Re*, polymer addition stabilises the flow. They also showed scalings for wall modes as $Re \sim \Sigma^{3/4}$ and for inviscid modes $Re \sim \Sigma^{1/2}$ for both the Newtonian fluid and viscoelastic fluid. Their numerical results showed that the inviscid modes for a Newtonian fluid can become unstable in plane Couette flow, which is in stark contrast to the results predicted by theory.[22] The first experimental verification of wall mode was accomplished by Verma and Kumaran.[23] They observed a wall mode scaling of $Re \sim \Sigma^{5/8}$, which deviates from theoretical prediction of $Re \sim \Sigma^{3/4}$, and they attributed this deviation to the plug-like (non-parabolic velocity distribution) flow at the centre due to deformation of the tube caused by the applied pressure gradient. After consideration of the modification of the base flow by the deformed tube, they were able to reconcile the wall mode scaling as $Re \sim \Sigma^{5/8}$ from theory to match with that of experiments. However, there was still a mismatch of critical Reynolds number between theory and experiments by a factor of 10. In a subsequent work,[24] they considered diverging and converging sections due to deformation in soft walls, and they were able to match pressure gradient with theory within experimental errors (10%). The other independent work of Neelamegam and Shankar[25] found a different scaling $Re \sim \Sigma^{3/2}$ but observed reduction in Reynolds number as low as 500 in the tube flow similar to Verma and Kumaran.[23] They could not arrive at a conclusion on whether the observed scaling is of wall mode or inviscid mode. The present state of the literature is that only wall modes are verified by both theory and experiments but inviscid modes are predicted by theory but are not observed in experiments so far.

Recent experiments of Srinivas and Kumaran[26] achieved a turbulent-like state in a deformable channel for Reynolds number range 250–400 comparable to high-*Re* turbulence in rigid channels. The above experiments are done with Newtonian fluid, and to the best of our knowledge, there is less work done on non-Newtonian fluids except for the recent work of Srinivas and Kumaran[7] in which they showed that small addition of polymer (dilute limit) having the mass fraction >1 decreased the critical Reynolds number (~30) considerably compared with the Newtonian fluid. Similarly, on the theoretical side, considerable amount of work has been done on the role of fluid elasticity on the instabilities in flow past a soft solid medium. Shankar and Kumar[27] studied the effect of viscoelasticity of the fluid on the stability of flow past a deformable solid in the creeping-flow limit for the first time and showed that the

unstable mode at finite Γ and Weissenberg number $W = \tau_R V/R$ (where τ_R is the relaxation time of the polymer) reduces to the stable Gorodtsov and Leonov (G-L) mode as a deformability parameter $\Gamma \to 0$ in the rigid case. When the wall is deformable, as one approaches the Newtonian fluid limit, the unstable mode reduces to the results of Kumaran *et al.*[22] as $W \to 0$. The results of this study were extended to high Re for the case of plane Couette flow of upper convected Maxwell fluid by Kumar and Shankar.[9] In their work, authors showed two distinct instability mechanisms for ZRGL (Zero Reynolds Gorodtsov and Leonov) modes and HFGL (High Frequency Gorodtsov and Leonov) modes. The ZRGL modes when continued to high Re show scaling of $\Gamma \propto Re^{-1/3}$ for a low Weissenberg number W, which is similar to Newtonian fluid, whereas the HFGL mode when continued to high Re shows scaling of $\Gamma \propto Re^{-1}$ for a finite Weissenberg number W. The above-mentioned studies on viscoelastic fluid have constant (shear-rate independent) viscosity, but relatively less attention has been paid to the role of shear-rate dependent viscosity on the stability of the flow.

The role of shear-rate dependence on the stability of fluid flow past a deformable surface was first addressed by Roberts and Kumar,[28] who carried out a stability analysis for a power-law fluid in plane Couette flow, considering the creeping-flow limit. They showed that for small values of solid thickness $H < 3$, the critical shear-rate Γ_c decreases with the increase in n, while for larger values of $H > 3$, Γ_c increases with n. The work of Pourjafar *et al.*[29] on the plane Poiseuille flow on Mooney-Rivlin solid showed that the flow becomes unstable in the creeping-flow limit, but the flow is stabilized compared with a Newtonian fluid for shear-thinning fluids ($n < 1$), but is destabilized for shear-thickening fluids ($n > 1$). They extended these results[30] to non-zero $Re \sim 10$ but only for shear-thinning fluids (with $n < 1$), and the flow is either stabilized or destabilized with the decrease in n depending on the Reynolds number. They further varied the ratio of the two Mooney-Rivlin elasticity constants and examined the effect on the stability. However, the authors did not provide any detailed scalings of the unstable mode (wall modes and/or inviscid modes) at high $Re \gg 1$. Further, the linearized interface conditions used in their work are slightly different from the interface conditions used in the work of Gaurav and Shankar.[31]

The focus of the present work is on the role of shear-rate dependence of the viscosity in a power-law fluid on the stability of flow past deformable solid surfaces, especially at high Re, with a goal to elucidate the physical origins of the scalings exhibited by unstable modes at high-Re. The rest of this paper is organised as follows: The formulation of the problem is discussed in Sec. II. We discuss the linear stability analysis for plane Couette flow of power-law fluid past a deformable solid in Sec. III. This is followed (in Sec. IV) by a detailed discussion on how shear-thinning/shear-thickening affects the stability. The salient conclusions of this work are summarized in Sec. V.

II. PROBLEM FORMULATION

The configuration of interest in this work is shown in Fig. 1, in which a power-law fluid occupies the region

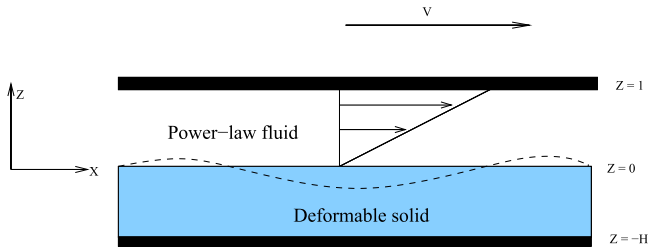

FIG. 1. Schematic representation of plane Couette flow of a power-law fluid past a deformable solid in the non-dimensional coordinate system.

$0 > z > R$ between the top rigid plate at $z = R$ and a deformable solid that occupies the region $0 < z < -HR$. The deformable solid is assumed to be perfectly bonded to the rigid plate at $z = -HR$. The top rigid plate moves with velocity V and the deformable solid is modelled as a neo-Hookean solid. The non-dimensional scheme followed in this problem is the same as that used by Roberts and Kumar.[28] The stress tensor for the power-law fluid in dimensional form (asterisk represents dimensional quantities) is given by

$$\mathbf{T}^* = -p_f^* \mathrm{I} + m^* \left(\frac{1}{2}\mathbf{II}_{\dot{\boldsymbol{\gamma}}}^*\right)^{\frac{(n-1)}{2}} \dot{\boldsymbol{\gamma}}^*, \tag{1}$$

$$\mathbf{T}^* = -p_f^* \mathrm{I} + \eta_{app}^* \dot{\boldsymbol{\gamma}}^*, \tag{2}$$

$$\dot{\boldsymbol{\gamma}}^* = \nabla \boldsymbol{v}^* + (\nabla \boldsymbol{v}^*)^{\mathrm{T}}, \qquad \mathbf{II}_{\dot{\gamma}}^* = -\frac{1}{2}[(\mathrm{Tr}\ \dot{\boldsymbol{\gamma}}^*)^2 - \left(\mathrm{Tr}\ \dot{\boldsymbol{\gamma}}^{*2}\right)]. \tag{3}$$

Here $\dot{\boldsymbol{\gamma}}$ is the rate-of-strain tensor and $\mathbf{II}_{\dot{\gamma}}^*$ is the second invariant of rate-of-strain tensor. The power-law fluid has a shear-rate dependent viscosity instead of a constant viscosity-like in the case of Newtonian fluid. The term $m^*\left(\frac{1}{2}\mathbf{II}_{\dot{\gamma}}^*\right)^{\frac{(n-1)}{2}}$ in the stress tensor is the (dimensional) apparent viscosity (η_{app}^*) and is dependent on the strain-rate of the fluid, where m^* is the consistency index in dimensional form. There is no obvious viscosity scale in the power-law model, whereas in the Carreau model, there is a well-defined zero-shear viscosity (viscosity in the limit of zero shear-rate). For this reason, we define a quantity η_f with dimensions of viscosity $\eta_f \equiv m^*/\hat{m}$, where $\hat{m}$ is chosen in such a way that η_f has dimensions of viscosity. This implies that $\hat{m}$ has dimensions of T^{n-1}, and the magnitude of $\hat{m}$ is fixed in the following discussion. We consider the following scales for nondimensionalizing the governing equations: lengths by R, time by η_f/G, and pressure and stresses by G (both for the solid and fluid). The non-dimensionalised governing equations and constitutive relation are given by

$$\nabla \cdot \mathbf{v} = 0, \tag{4}$$

$$\frac{Re}{\Gamma}\frac{D\boldsymbol{v}}{Dt} = -\nabla p_f + \nabla \cdot \boldsymbol{\tau}, \tag{5}$$

$$\boldsymbol{\tau} = \hat{m}\left(\frac{G}{\eta_f}\right)^{n-1}\left(\frac{1}{4}\mathrm{Tr}\ \dot{\boldsymbol{\gamma}}^2\right)^{\frac{(n-1)}{2}}\dot{\boldsymbol{\gamma}} = m\left(\frac{1}{4}\mathrm{Tr}\ \dot{\boldsymbol{\gamma}}^2\right)^{\frac{(n-1)}{2}}\dot{\boldsymbol{\gamma}}, \tag{6}$$

where $\Gamma = \frac{V\eta_f}{GR}$ is the non-dimensional strain-rate in the fluid and $m = \hat{m}\left(\frac{G}{\eta_f}\right)^{(n-1)}$ is the non-dimensional consistency index. In our analysis, we set the nondimensional quantity $m = 1$,

which fixes $\hat{m} = \left(\frac{m^*}{G}\right)^{(1-\frac{1}{n})}$ unambiguously using the experimentally evaluated values of m^* and n.

The solid is modeled as a neo-Hookean solid using Lagrangian three-state formulation similar to that of Chokshi and Kumaran.[32] Undeformed, pre-stressed (deformed base-state), and perturbed states are important in the Lagrangian three-state formulation for stability analysis, whereas Gkanis and Kumar[33] modeled the neo-Hookean solid using two-state Lagrangian formulation in which only undeformed and perturbed states are important for stability analysis. Chokshi and Kumaran[32] showed in their work that two-state Lagrangian, three-state Lagrangian, and Eulerian formulation stability results of Couette flow agree with the creeping-flow limit. The particle motion in the solid is given by

$$\mathbf{x}(\mathbf{X}, t) = \mathbf{X} + \mathbf{u}(\mathbf{X}, t), \tag{7}$$

where $\mathbf{X} = (X_1, X_2, X_3)$ is the reference position of a material particle at time $t = 0$, $\mathbf{x} = (x_1, x_2, x_3)$ is the current position of particle at any time t, and $\mathbf{u} = (u_1, u_2, u_3)$ is the displacement vector of the particle. The deformation gradient tensor of solid relating the reference position and current position is given as

$$\det(\mathbf{F}) = 1, \quad \mathbf{F} = \frac{\partial \mathbf{x}}{\partial \mathbf{X}}, \tag{8}$$

where $\mathbf{F}$ is the Lagrangian deformation gradient tensor in the solid. The Cauchy stress tensor for neo-Hookean elastic solid is given by[33,34]

$$\boldsymbol{\sigma} = -p_g \mathbf{I} + G\,\mathbf{F} \cdot \mathbf{F}^T. \tag{9}$$

The non-dimensionalised momentum balance equation for neo-Hookean solid is

$$\frac{Re}{\Gamma}\frac{\partial^2 \boldsymbol{u}}{\partial t^2} = \nabla_{\mathbf{X}} \cdot \mathbf{P}, \quad \mathbf{P} = \mathbf{F}^{-1} \cdot \boldsymbol{\sigma}, \tag{10}$$

where $\mathbf{P}$ is the first Piola-Kirchhoff stress tensor. The base-state velocity and deformation for the fluid and solid are

$$\overline{\boldsymbol{v}} = (\Gamma z, 0, 0), \quad \overline{\boldsymbol{u}} = [\mu\Gamma^n (X_3 + H), 0, 0], \tag{11}$$

where $\mu = m(1/2)^{\frac{(n-1)}{2}}$ and $m = \hat{m}\left(\frac{G}{\eta_f}\right)^{(n-1)}$ is set to 1 in our analysis.

III. LINEAR STABILITY ANALYSIS

The stability of plane Couette flow of a power-law fluid is studied by imposing infinitesimally small perturbations on the base state, and the corresponding governing equations of fluid and deformable solid are linearised. In this work, we consider only two-dimensional perturbations that in the normal mode form is given as

$$f' = \tilde{f}(z) \exp[ik(x - ct)], \tag{12}$$

where f' is any dynamical quantity in the fluid and solid, $\tilde{f}(z)$ is the amplitude, k is the wavenumber, and c is the wave speed, which is a complex-valued quantity for temporal stability analysis. The linearised perturbation equations for power-law fluid are

$$D\tilde{v}_z + ik\tilde{v}_x = 0, \tag{13}$$

$$-ik\tilde{p}_f + \mu\Gamma^{(n-1)}[(D^2 - k^2) + (n-1)(ikD + D^2)]\tilde{v}_x + \mu\Gamma^{(n-1)}(n-1)[ikD - k^2]\tilde{v}_z = \frac{Re}{\Gamma}[ik\tilde{v}_x(\Gamma z) - ikc\tilde{v}_x + \Gamma\tilde{v}_z], \tag{14}$$

$$-D\tilde{p}_f + \mu\Gamma^{(n-1)}[(n-1)(D^2 + ikD)]\tilde{v}_x + \mu\Gamma^{(n-1)}[ikD - k^2]\tilde{v}_z = \frac{Re}{\Gamma}[ik(\Gamma z - c)]\tilde{v}_z. \tag{15}$$

The relation between pre-stressed and current positions for the material particle, after applying perturbations, is considered as follows:

$$\mathbf{x}(\mathbf{X}, t) = \bar{\mathbf{x}}(\mathbf{X}) + \mathbf{u}'(\bar{\mathbf{x}}, t). \tag{16}$$

The deformation gradient tensor relating pre-stressed state and current position is[32]

$$\mathbf{F} = \frac{\partial \mathbf{x}}{\partial \bar{\mathbf{x}}} \cdot \frac{\partial \bar{\mathbf{x}}}{\partial \mathbf{X}} = \mathbf{F}' \cdot \overline{\mathbf{F}}. \tag{17}$$

The incompressibility and momentum balance equations, after imposing perturbations, are given as

$$\det(\mathbf{F}') = 1, \qquad \frac{Re}{\Gamma}\frac{\partial^2 \boldsymbol{u}}{\partial t^2} = \nabla_{\bar{\mathbf{x}}} \cdot \mathbf{P}. \tag{18}$$

The linearized equations for the solid in Lagrangian three-state formulation are given by

$$D\tilde{u}_3 + ik\tilde{u}_1 = 0, \tag{19}$$

$$-ik\tilde{p}_g + (D^2 - k^2)\tilde{u}_1 - k^2\Gamma^{2n}\mu^2\tilde{u}_1 - 2\Gamma^n ik\mu D\tilde{u}_1 + \frac{Re}{\Gamma}k^2c^2\tilde{u}_1 = 0, \tag{20}$$

$$-D\tilde{p}_g + (D^2 - k^2)\tilde{u}_3 - k^2\Gamma^{2n}\mu^2\tilde{u}_3 - 2\Gamma^n ik\mu D\tilde{u}_3 + \frac{Re}{\Gamma}k^2c^2\tilde{u}_3 = 0, \tag{21}$$

where $D = \frac{d}{d\bar{x}_3}$.

At $z = 0$, i.e., at the fluid-solid interface, the linearised boundary conditions are

$$\tilde{v}_x + \Gamma\tilde{u}_3 + ikc\,\tilde{u}_1 = 0, \tag{22}$$

$$\tilde{v}_z + ikc\,\tilde{u}_3 = 0, \tag{23}$$

$$(D\tilde{u}_1 + ik\tilde{u}_3) - \mu\Gamma^{(n-1)}n(D\tilde{v}_x + ik\tilde{v}_z) = 0, \tag{24}$$

$$\tilde{p}_g - 2D\tilde{u}_3 + 2ik\Gamma^n\,\tilde{u}_3 - \tilde{p}_f + 2\mu\Gamma^{(n-1)}D\tilde{v}_z = 0. \tag{25}$$

No-slip and no-penetration conditions are applied at top and bottom rigid plates,

$$\tilde{v}_z = 0, \quad \tilde{v}_x = 0 \quad \text{at} \quad z = 1, \tag{26}$$

$$\tilde{u}_3 = 0, \quad \tilde{u}_1 = 0 \quad \text{at} \quad z = -H. \tag{27}$$

The linearised differential equations for each medium together with boundary conditions form an eigenvalue problem, which is of the form

$$c^2\,\mathbf{A}\,\mathbf{x} + c\,\mathbf{B}\,\mathbf{x} + \mathbf{C}\,\mathbf{x} = 0. \tag{28}$$

The eigenvalue problem (for c) is solved numerically using the pseudospectral method.[35] This numerical method has the issue of producing spurious eigenvalues along with the genuine eigenvalues. This is overcome by taking two different values of the number of collocation points and by filtering out the

genuine eigenvalues obtained from the two sets. The eigenvalues that are computed numerically provide information about the stability of the system. If the imaginary part of wave speed is $c_i < 0$, then the flow is stable, if $c_i > 0$, the flow is unstable, and for $c_i = 0$, the flow is neutrally stable. The real part of wave speed gives information about oscillatory nature of eigenvalues, i.e., its phase speed. To get the results in the pertinent parametric regime, the respective unstable eigenmode is tracked using shooting method.[36]

IV. RESULTS

Before discussing the results of present work, it is appropriate to recapitulate the results obtained in the earlier studies[28] for power-law fluid past a neo-Hookean solid in the creeping-flow limit. Roberts and Kumar[28] showed that the variation of minimum strain-rate (Γ_c) required to destabilise the flow with thickness (H). This followed a non-monotonic nature with change in power-law index n. Shear-thinning fluids ($n < 1$) show stabilization, predicting higher Γ_c at low H, but show destabilization predicting lower Γ_c at high H when compared with a Newtonian fluid. Shear-thickening fluids ($n > 1$) show the exact opposite behavior when compared with shear-thinning fluids. The present work is an extension of the earlier work[28] to finite and high Re. In a power-law fluid, the viscosity is not constant like in the case of a Newtonian fluid and the viscosity (apparent viscosity) changes with strain-rate. In Sec. III, we briefly mentioned the numerical method used to solve the problem, and we show here that the convergence of numerical (pseudospectral) method for different collocation points N varies from 35 to 75 and points, $N > 60$ showed the converged eigenvalue to the tenth decimal point as shown in Fig. 2(a). Neutral stability curves Γ vs k for which the imaginary part of wave speed is zero ($c_i = 0$) are plotted, which gives information about the minimum strain-rate (Γ_c) required to destabilise the flow as shown in Fig. 2(b). We first validated our results with the earlier rigid surface results.[16] To this end, we reproduced the spectrum from the work of Liu and Liu[16] for the case of $n = 0.2$ at $Re = 1000$, but they considered two rigid plates moving in opposite directions. In order to facilitate comparison of their spectrum with our case (where we considered bottom rigid plate to be stationary), we have shown the comparison of the spectra between two plates moving in opposite directions and only top-plate moving as shown in Figs. 3(a) and 3(b). To benchmark our results with deformable solid, we consider the same parameters as that of the rigid case and obtain the rigid spectrum from deformable solid spectrum in three different ways: first, making the shear modulus of deformable solid very high, i.e., $\Gamma \to 0$; second, reducing the thickness of a deformable solid, $H \to 0$; and third, by reducing

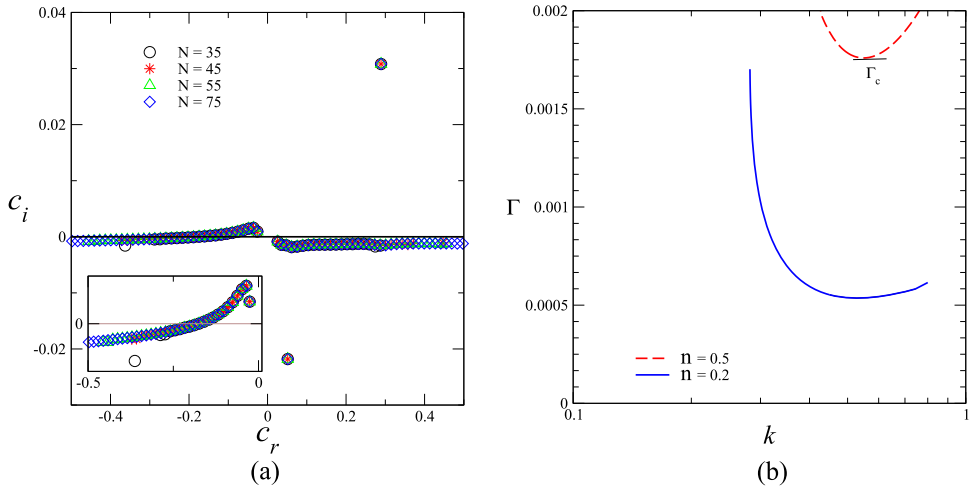

FIG. 2. (a) Convergence of the spectrum with different collocations points N for the parameter set $Re = 1000$, $H = 10$, $n = 0.2$, $m = 1$, and $\Gamma = 0.5$. (b) Neutral stability curves in Γ-k plane for different values of n for the parameter set $Re = 10\,000$, $m = 1$, and $H = 10$.

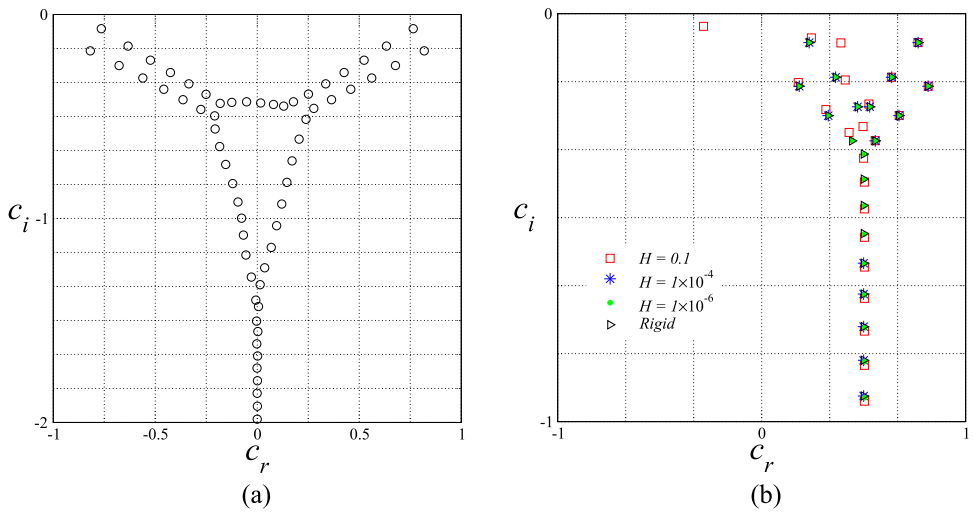

FIG. 3. (a) Comparison of rigid surface spectrum obtained in this work with the results of Liu and Liu[16] for the parameter set $Re = 1000$, $n = 0.2$, and $m = 1$, with top and bottom rigid plates moving in opposite directions. (b) Limit of rigid surface spectrum (only top-plate moving) as obtained from the deformable solid spectrum for the parameter set $Re = 1000$, $n = 0.2$, $\Gamma = 1$, and $m = 1$ at different thicknesses H, for $H \ll 1$.

TABLE I. Validation of the present results with the results of Roberts and Kumar[28] where Γ_c and k_c are critical values for the instability obtained from neutral stability curves. The results of Roberts and Kumar were obtained by our numerical code.

		Present results ($Re = 1 \times 10^{-4}$)		Roberts and Kumar ($Re = 0$)	
n	H	Γ_c	k_c	Γ_c	k_c
$n = 0.3$	1	0.336 687 287	4.453 516 86	0.336 687 552	4.453 5168 6
$n = 0.3$	5	0.141 247 357	0.645 000 20	0.141 247 579	0.463 064 42
$n = 0.3$	10	0.040 240 947	0.249 334 86	0.040 240 935	0.249 334 86
$n = 0.5$	5	0.402 515 379	0.463 064 42	0.402 515 768	0.463 064 42
$n = 0.5$	10	0.130 526 550	0.209 756 75	0.130 526 431	0.209 756 75

together ($\Gamma, H \to 0$). We choose thickness of the deformable solid varying from $H = 0.1$ to 1×10^{-6} and we observe that at $H = 1 \times 10^{-4}$, the deformable solid spectrum matches with that of the rigid spectrum with only the top-plate moving as shown in Fig. 3(b). To validate our results with that of Roberts and Kumar,[28] we compared our results obtained from our numerical code at $Re = 10^{-4}$ with those of Roberts and Kumar[28] in the creeping-flow limit and found good agreement as shown in Table I. This validates our numerical results for a deformable solid with the results of rigid surface and deformable solid in the creeping-flow limit.

The main goal of the present work is to examine how shear-thinning/shear-thickening affects the wall modes present in the flow of a Newtonian fluid. First, we consider the case of shear-thickening fluid and we track the finite-wave mode present in the creeping-flow limit to high Re and compare this with the results obtained for a Newtonian fluid. As the power-law index n increases above one, our results show higher Γ [as shown in Fig. 4(a)] for the flow as well as different scalings compared with a Newtonian fluid. Results for $n = 1.5$ show a scaling of $\Gamma \sim Re^{-0.25}$, and for $n = 1.75$, results show scaling of $\Gamma \sim Re^{-0.22}$, which can be seen from Fig. 4(b). Similarly, shear-thinning fluids also show different scalings for the wall modes. For $n = 0.8$, results show scaling of $\Gamma \sim Re^{-0.38}$, and the results of $n = 0.5$ show a scaling of $\Gamma \sim Re^{-0.5}$, which can be seen from Fig. 4(d). This demonstrates that for different n values, Γ scales differently with Re. Previous studies[21] showed that for a Newtonian fluid, the wall modes scale as $\Gamma \sim Re^{-1/3}$ at $Re \gg 1$, and our numerical results for the case of $n = 1$ also confirm the same scaling as shown in Fig. 4(b). To understand why different scalings occur for different n values, motivated by the wall mode scaling in a Newtonian fluid, we postulate the scaling in a power-law fluid based on the apparent viscosity (η_{app}), which follows scaling $\Gamma_{app} \sim Re^{-1/3}$, where $\Gamma_{app} = \frac{V\eta_{app}}{GR}$, and the "apparent" viscosity is the actual viscosity of the fluid, which changes with strain-rate, but it is important to note the

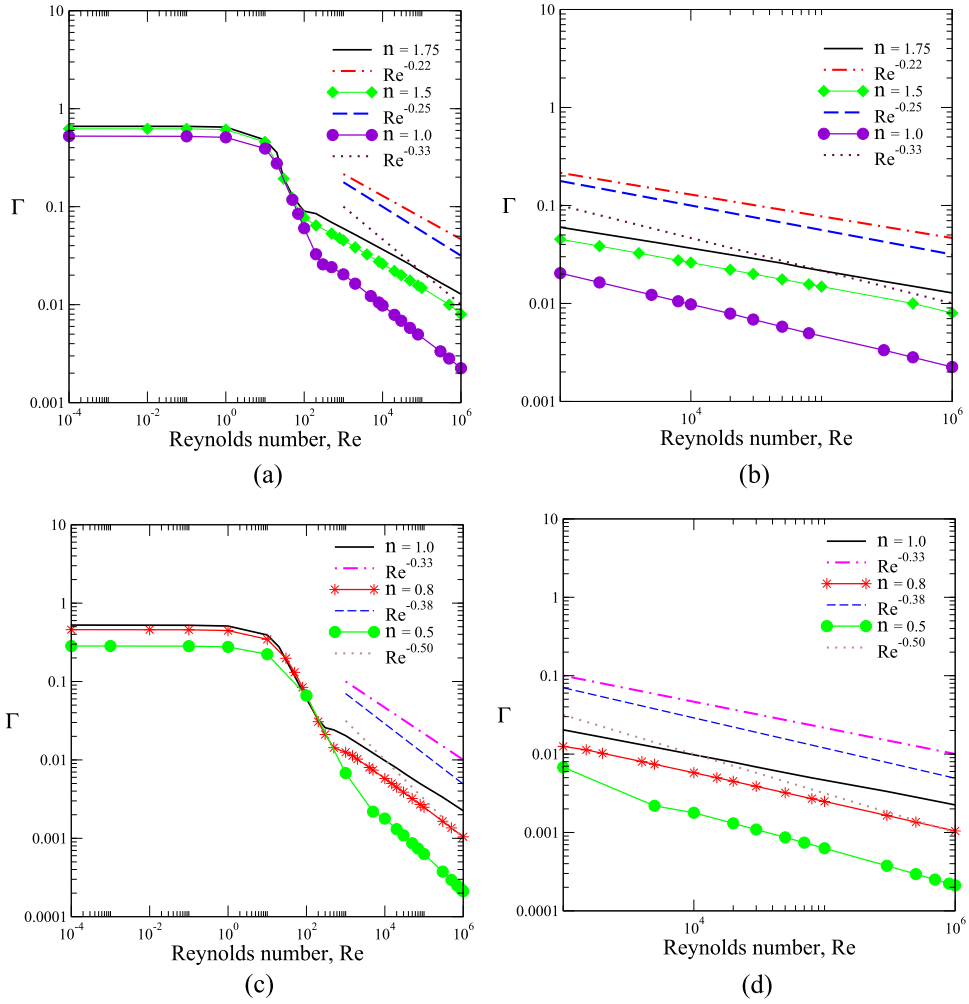

FIG. 4. Plane Couette flow past a deformable solid: (a) non-dimensional strain-rate (Γ) as a function of Reynolds number (Re) for different values of $n > 1$, and (b) the plot (a) is zoomed in for high Re. (c) Γ as a function of Reynolds number (Re) for different values of $n < 1$, and (d) the plot (c) is zoomed in for high Re.

difference that the strain-rate ($\Gamma = \frac{V\eta_f}{GR}$) definition based on a constant Newtonian-like viscosity (η_f). The viscous forces are dominant in the boundary layer $\delta \ll 1$ near the wall, similar to that of a Newtonian fluid. The fluid domain is split into inner and outer wall layers. The inner wall layer is of thickness $z = \xi\delta$ where viscous forces are dominant, and in the outer layer, viscous forces are negligible at high Re. Based on the inner layer, the base state velocity profile according to the inner variable ξ can be written as $U(z) = \Gamma z = \Gamma\xi\delta$. The derivatives in the wall layer are transformed as $d_\xi = \delta^{-1}d_z$. Now, the continuity and momentum equations are rewritten in terms of inner variable ξ. To estimate the scaling of boundary layer thickness δ, the x-momentum equation is considered.

After rescaling Eq. (14), the viscous and inertial terms of the equation are balanced in the wall layer to give

$$\Gamma^{(n-1)}\frac{1}{\delta^2}d^2_{\xi^2}\tilde{v}_z \sim Re[ik\tilde{v}_x(U - \frac{c}{\Gamma}) + \tilde{v}_z]. \tag{29}$$

The right-hand side term in Eq. (29) is of $O(\delta)$ (since $U \sim \frac{c}{\Gamma} \sim \delta$), then $\Gamma^{(n-1)} \sim Re\delta^3$, and after rearranging, the scaling for boundary layer thickness is given by

$$\delta \sim \left(\frac{\Gamma^{(n-1)}}{Re}\right)^{1/3}. \tag{30}$$

We postulate that scaling for the wall modes for a power law fluid is obtained by balancing the viscous stresses in the wall layer with elastic stress in the solid: $\frac{V\eta_{app}}{\delta R} \sim G$, where η_{app} is the viscosity corresponding to the shear-rate in the base flow. After substituting δ from Eq. (30) into the stress balance, we obtain

$$\frac{V\eta_f\hat{m}\dot{\gamma}^{(n-1)}}{R\left(\frac{\Gamma^{(n-1)}}{Re}\right)^{(1/3)}} \sim G, \tag{31}$$

$$\frac{\dot{\gamma}\eta_f}{G}\hat{m}\dot{\gamma}^{(n-1)} \sim \Gamma^{(n-1)/3}Re^{\frac{-1}{3}}$$

$$\Rightarrow \quad \Gamma^{1+\frac{2(n-1)}{3}} \sim Re^{\frac{-1}{3}} \text{ (since } \Gamma = \frac{\dot{\gamma}\eta_f}{G}\text{)}.$$

The final scaling that we obtain based on the shear-rate dependent viscosity is given by

$$\Gamma \sim Re^{\frac{-1}{2n+1}}. \tag{32}$$

The scaling obtained from numerics is next compared with the above theoretical scaling. For the case of $n = 1.5$, from theory, we predict $\Gamma \sim Re^{-1/4}$, and from numerics, we obtain $\Gamma \sim Re^{-0.25}$.

For the other cases, scalings are given in Table II, and it is clearly seen that numerical results agree well with the theoretical prediction. The scaling derived for Γ from Eq. (32) is substituted back into Eq. (30) and then the final scaling obtained for boundary layer thickness is given by

$$\delta \sim Re^{\frac{-n}{2n+1}}. \tag{33}$$

Numerically evaluated boundary layer thickness when plotted as a function of Re follows the theoretical boundary layer scaling [Eq. (33)], which can be seen in Fig. 5. For the case of $n = 1$, the eigenfunction is plotted as shown in Fig. 6(b), and it shows that close to the fluid-solid interface, there is a sharp variation in perturbed velocity and it becomes zero at rigid surface indicating that the behaviour of eigenfunction is typical of wall modes, similar to the Newtonian results of Shankar and Kumaran.[21] Another characteristic feature of wall mode is that $\frac{c_r}{\Gamma}$ shows scaling, which is a function of Re, and the same behaviour can be seen for both shear-thickening and shear-thinning fluids having power-law index $n > 0.3$ in Fig. 6(a).

TABLE II. Γ vs Re^α for different values of power-law index n, for $Re \ll 1$.

Power-law index, n	α (theory)	α (numerics)
$n = 1.75$	$-2/9$	-0.22
$n = 1.5$	$-1/4$	-0.25
$n = 1.0$	$-1/3$	-0.33
$n = 0.8$	$-5/13$	-0.38
$n = 0.5$	$-1/2$	-0.50
$n = 0.25$	$-2/3$	-1.0
$n = 0.2$	$-5/7$	-1.0

A. Inviscid mode

For the case of $n = 0.25$, the plot of strain-rate (Γ) as a function of Reynolds number shows a scaling of $\Gamma \sim Re^{-1}$, which deviates from wall modes scaling $\Gamma \sim Re^{-2/3}$ (as predicted by theory) as can be seen in Fig. 7(a). Similarly for $n = 0.2$, results show numerical scaling $\Gamma \sim Re^{-1}$, but from theoretical scaling, it should be $\Gamma \sim Re^{-5/7}$. It is well known[37] that for wall modes, $\frac{c_r}{\Gamma} \to 0$, and for inviscid modes, $\frac{c_r}{\Gamma} \sim O(1)$ for plane channel flow. To understand this departure from wall mode for $n = 0.2$ and 0.25, we have plotted c_r/Γ vs Re, which does not scale with Re, and it remains $O(1)$ (inviscid mode behaviour) as shown in Fig. 7(b); whereas, for wall modes, c_r/Γ decreases with Re as can be seen from Fig. 6(a). From this, we conclude that scaling is indeed an inviscid mode scaling. The question then arises regarding the existence of the wall mode instability for cases $n = 0.2$ and 0.25. From the previous work, it is

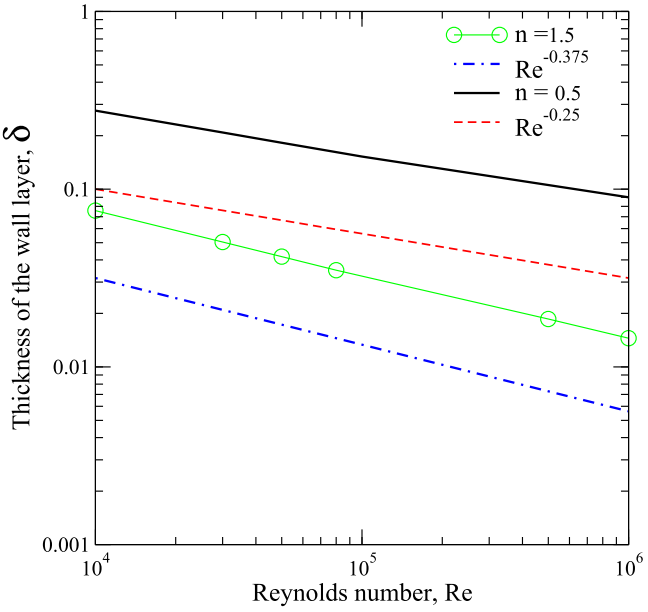

FIG. 5. Comparison of numerically evaluated boundary layer thickness with that of theory for different values of n as a function of Re.

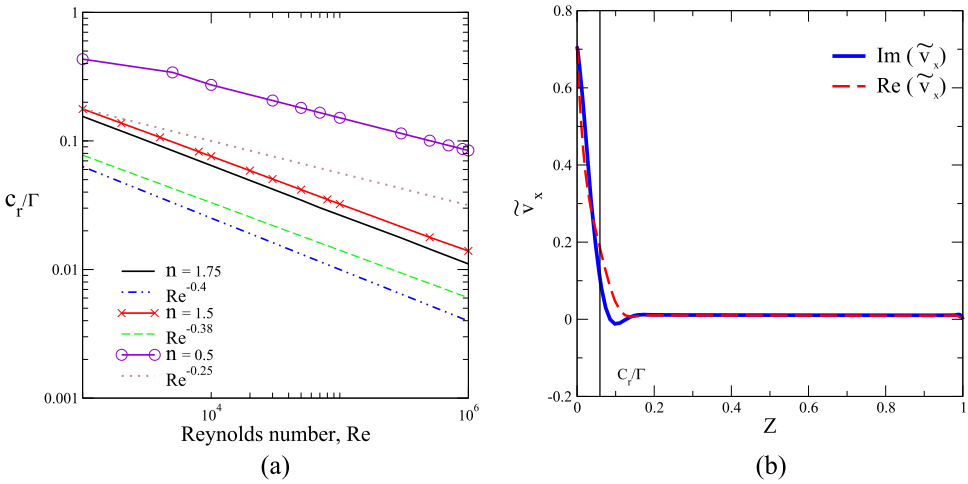

FIG. 6. (a) Scaling of c_r/Γ with Re for different shear-thickening fluids. (b) Eigenfunction is plotted to show boundary layer formation near the wall for $n = 1$.

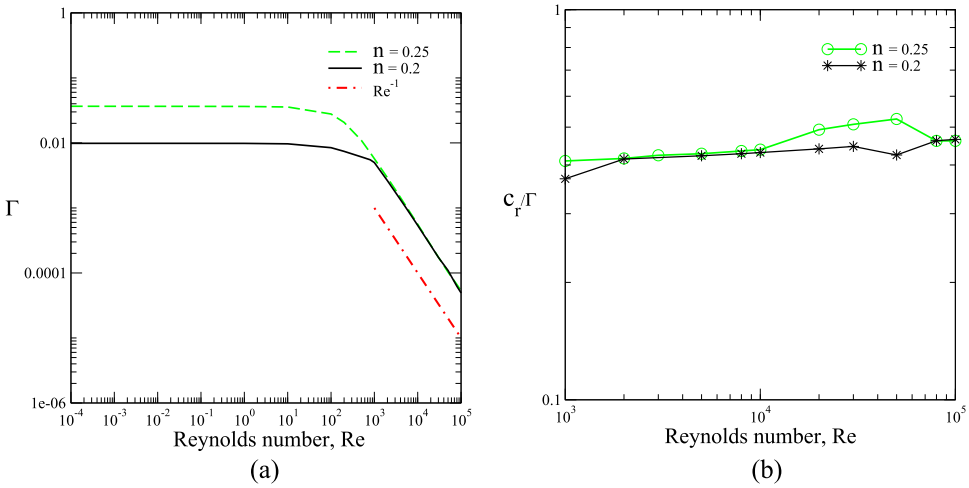

FIG. 7. (a) Non-dimensional strain-rate as a function of Reynolds number (Re) for values of $n = 0.2$ and $n = 0.25$. (b) Scaling of c_r/Γ with Re for $n = 0.2$ and $n = 0.25$.

known that the inviscid mode is the most unstable one compared with the wall mode at high Re, so one might expect that the wall mode should be present at a higher Γ value, but we did not observe any unstable wall mode. Instead, we observe multiple inviscid modes with scaling $\Gamma \sim Re^{-1}$. By careful observation, we found that the finite-wave mode present in the creeping-flow limit, when continued to high Re, transforms to the inviscid mode for $n \leq 0.3$, but the same finite-wave mode transforms to the wall mode for $n > 0.3$. Therefore, it is concluded that there is no wall mode instability for $n \leq 0.3$, and because of this reason, scalings do not follow the predictions from the wall mode theory.

Similar features are reflected in the creeping-flow results of Roberts and Kumar[28] in which critical strain-rate (Γ_c) was plotted as a function of non-dimensional thickness, H, and they showed a very distinct behaviour for power-law index values $n > 0.5$ and $n < 0.5$. For $n > 0.5$ at low H, shear-thinning fluid stabilises the flow, and at high H, it destabilises the flow when compared with the Newtonian fluid. Similarly, shear-thickening fluids show an exact opposite behaviour from that of shear-thinning fluids. This behaviour of finite-wave mode in the creeping-flow limit, when extended to high Re, shows wall-mode scaling in our results. Roberts and Kumar[28] also showed in their results that when the value of n is changed from 0.5 to 0.3, the critical strain-rate shows always destabilisation when compared with the Newtonian fluid, and when that finite-wave mode is tracked to high Re, it exhibits inviscid-mode scaling.

Eigenfunctions are plotted to demonstrate the boundary layer structure near the wall at high Reynolds number. In the previous work,[21] for wall modes, it was shown that a sharp variation in both the stream-wise and normal velocity eigenfunctions is observed near the fluid-solid interface as shown in Fig. 6(b), but the velocity eigenfunction decays quickly to zero in the bulk and is zero all the way up to the top rigid wall. Compared with the Newtonian case, for shear-thickening fluids, the boundary layer thickness near the wall decreases and for shear thinning fluids, boundary layer thickness near the wall increases as shown in Figs. 8(a)–8(d). For the case of $n \leq 0.3$, the eigenfunction does not show a sharp variation of velocity near the interface and the structure of the eigenfunction is very different from the wall mode eigenfunction [Figs. 8(d) and 9(a)], which further lends support to the hypothesis that the unstable mode is an inviscid mode. Inviscid mode instability, which is present in the Newtonian fluid[8] is predicted at high Re. Hence Chokshi and Kumaran[8] argued that the viscoelastic nature of the fluid (UCM, Oldroyd-B) does not affect the inviscid mode present in the Newtonian fluid. But we observed that the shear-rate dependent viscosity of a power-law fluid does affect the inviscid mode instability present in the Newtonian fluid. Shear-thinning/shear-thickening nature of power-law fluid can stabilise/destabilise the inviscid mode

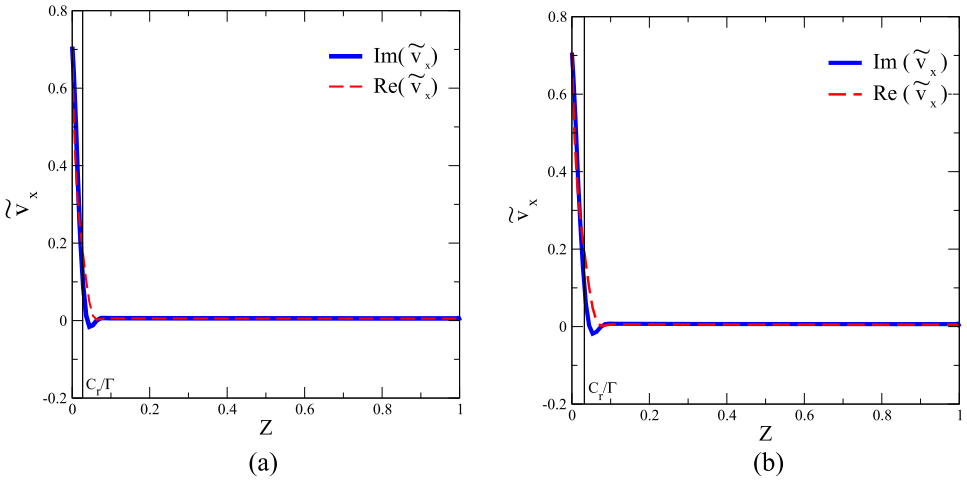

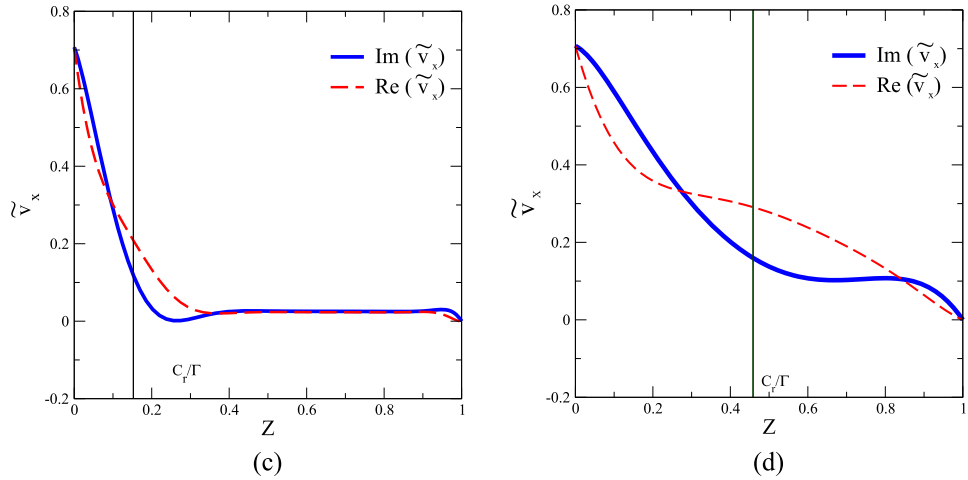

FIG. 8. Eigenfunctions are plotted to show boundary layer formation near the wall for shear-thickening and shear-thinning fluids for the parameters H = 10, k = 0.5, m = 1, and Re = 10^5 for (a) n = 1.75, (b) n = 1.5, (c) n = 0.5, and (d) n = 0.3.

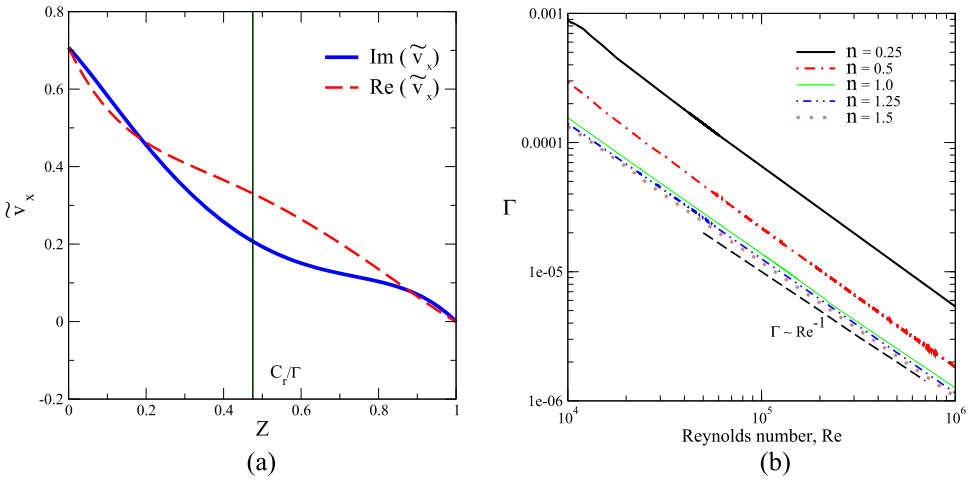

FIG. 9. Eigenfunctions are plotted to show boundary layer formation near the wall for shear-thinning fluids for the parameters H = 10, k = 0.5, m = 1, and Re = 10^5 for (a) n = 0.2 and (b) non-dimensional strain-rate as a function of Re for the parameters H = 10, m = 1, and k = 1.5.

when compared with the Newtonian fluid, which can be seen in Fig. 9(b).

V. CONCLUSIONS

Linear stability analysis is carried out for plane Couette flow of a power-law fluid past a deformable (neo-Hookean) solid at arbitrary Re to analyse the effect of shear-thinning/shear-thickening on the two modes of instability (wall mode and inviscid mode) present in the Newtonian fluid. At high Re, the unstable wall modes in a power law fluid show different scalings (in the pertinent parametric space of Γ vs Re) compared with the Newtonian case, with different scaling exponents for different values of power-law index (n). Based on the understanding of wall modes in a Newtonian fluid, wherein viscous stresses in the wall layer and solid elastic stresses are balanced to arrive at the scaling, we proposed a theoretical scaling for power-law fluid, which is based on the actual viscosity (η_{app}) of the fluid (at the shear rate corresponding to the laminar flow), and not on the Newtonian-like constant viscosity (η_f). We show that a balance of the viscous stresses in the wall layer based on the actual

(shear-rate-dependent) viscosity with the solid elastic stresses yields the numerically observed scaling of $\Gamma \sim Re^{\frac{-1}{2n+1}}$. The numerically evaluated boundary layer thickness δ for wall modes agrees with the theoretically expected scaling $\delta \sim Re^{\frac{-n}{2n+1}}$ for wall modes when $n > 0.3$. However, in the numerical results, we observed a deviation from wall mode scaling for $n < 0.3$, wherein our results indicate that $\Gamma \propto Re^{-1}$, and $\frac{c_r}{\Gamma} \sim O(1)$ (as opposed to $\frac{c_r}{\Gamma} \sim Re^{-1/3}$ for wall modes), which is a characteristic exhibited by inviscid modes. The structure of eigenfunctions also supports this inference: for $n > 0.3$, the value of the power-law index (n) decreases as the boundary layer thickness near the wall increases. For $n < 0.3$, the eigenfunctions do not show sharp variations near the wall reinforcing the conclusion that the unstable modes are inviscid modes for $n < 0.3$. The power-law index n affects the stability of inviscid modes indicating that a change in the value of n can stabilize/destabilize the inviscid modes. For shear-thinning fluids ($n < 1$), results show higher Γ values for instability whereas the results of shear-thickening fluids ($n > 1$) show lower Γ values for instability, which is opposite to the behaviour observed for wall modes. The power-law model overpredicts viscosity at low and high strain-rates, and hence, more accurate models like the Carreau model can be employed to determine the stability of non-Newtonian fluids past deformable solids, but the results are likely to remain qualitatively similar to the results predicted by the power-law model in this study. The present study thus shows that shear-rate dependence of the viscosity has a marked effect on the stability characteristics of plane Couette flow past a deformable solid. Further, for $n < 0.3$, the only mode that is predicted is the inviscid instability, which is a more powerful destabilizing mechanism, and this prediction is therefore relevant to the flow of many commonly encountered shear-thinning fluids, which typically have $n < 0.25$.

[1] J. C. McDonald and G. M. Whitesides, "Poly(dimethylsiloxane) as a material for fabricating microfluidic devices," Acc. Chem. Res. **35**, 491–499 (2002).
[2] G. M. Whitesides, "The origins and the future of microfluidics," Nature **442**, 368 (2006).
[3] A. D. Stroock, S. K. W. Dertinger, and A. Ajdari, "Chaotic mixer for microchannels," Science **295**, 647–651 (2002).
[4] A. D. Stroock, S. K. W. Dertinger, G. M. Whitesides, and A. Ajdari, "Patterning flows using grooved surfaces," Anal. Chem. **74**, 5306–5312 (2002).
[5] V. Hessel, H. Lowe, and F. Schonfeld, "Micromixers—A review on passive and active mixing principles," Chem. Eng. Sci. **60**, 2479–2501 (2005).
[6] V. Kumaran and P. Bandaru, "Ultra-fast microfluidic mixing by soft-wall turbulence," Chem. Eng. Sci. **149**, 156–168 (2016).
[7] S. S. Srinivas and V. Kumaran, "Effect of viscoelasticity on the soft-wall transition and turbulence in a microchannel," J. Fluid Mech. **812**, 1076–1118 (2017).
[8] P. Chokshi, P. Bhade, and V. Kumaran, "Wall-mode instability in plane shear flow of viscoelastic fluid over a deformable solid," Phys. Rev. E **91**, 023007 (2015).
[9] A. S. Kumar and V. Shankar, "Instability of high-frequency modes in viscoelastic plane Couette flow past a deformable wall at low and finite Reynolds number," J. Non-Newtonian Fluid Mech. **125**, 121–141 (2005).
[10] V. A. Romanov, "Stability of plane-parallel Couette flow," Funct. Anal. Appl. **7**, 137–146 (1973).
[11] N. D. Waters, "The stability of two stratified power-law liquids in Couette flow," J. Non-Newtonian Fluid Mech. **12**, 85–94 (1983).
[12] B. Khomami, "Interfacial stability and deformation of two stratified power law fluids in plane poiseuille flow: Part I. Stability analysis," J. Non-Newtonian Fluid Mech. **36**, 289–303 (1990).
[13] B. Khomami, "Interfacial stability and deformation of two stratified power law fluids in plane poiseuille flow: Part II. Interface deformation," J. Non-Newtonian Fluid Mech. **37**, 19–36 (1990).
[14] C. Nouar, A. Bottaro, and J. P. Brancher, "Delaying transition to turbulence in channel flow: Revisiting the stability of shear-thinning fluids," J. Fluid Mech. **592**, 177–194 (2007).
[15] V. Chikkadi, A. Sameen, and R. Govindarajan, "Preventing transition to turbulence: A viscosity stratification does not always help," Phys. Rev. Lett. **95**, 264504 (2005).
[16] R. Liu and Q. Liu, "Non-modal instabilities of two-dimensional disturbances in plane Couette flow of a power-law fluid," J. Non-Newtonian Fluid Mech. **165**, 1228–1240 (2010).
[17] R. Liu and Q. S. Liu, "Non-modal instability in plane Couette flow of a power-law fluid," J. Fluid Mech. **676**, 145–171 (2011).
[18] R. Liu and Q. S. Liu, "Nonmodal stability in hagen-poiseuille flow of a shear thinning fluid," Phys. Rev. E **85**, 066318 (2012).
[19] V. Kumaran, "Effect of fluid flow on the fluctuations at the surface of an elastic medium," J. Chem. Phys. **102**, 3452 (1994).
[20] V. Kumaran, "Stability of the flow of a fluid through a flexible tube at high Reynolds number," J. Fluid Mech. **302**, 117–139 (1995).
[21] V. Shankar and V. Kumaran, "Stability of wall modes in fluid flow past a flexible surface," Phys. Fluids **14**, 2324–2338 (2002).
[22] V. Kumaran, G. H. Fredrickson, and P. Pincus, "Flow induced instability of the interface between a fluid and a gel at low Reynolds number," J. Phys. II France **4**, 893–904 (1994).
[23] M. K. S. Verma and V. Kumaran, "A dynamical instability due to fluid-wall coupling lowers the transition Reynolds number in the flow through a flexible tube," J. Fluid Mech. **705**, 322–347 (2012).
[24] M. K. S. Verma and V. Kumaran, "Stability of the flow in a soft tube deformed due to an applied pressure gradient," Phys. Rev. E **91**, 043001 (2015).
[25] R. Neelamegam and V. Shankar, "Experimental study of the instability of laminar flow in a tube with deformable walls," Phys. Fluids **27**, 024102 (2015).
[26] S. S. Srinivas and V. Kumaran, "After transition in a soft-walled microchannel," J. Fluid Mech. **780**, 649–686 (2015).
[27] V. Shankar and S. Kumar, "Instability of viscoelastic plane Couette flow past a deformable wall," J. Non-Newtonian Fluid Mech. **116**, 371–393 (2004).
[28] S. A. Roberts and S. Kumar, "Stability of creeping Couette flow of power-law fluid past a deformable solid," J. Non-Newtonian Fluid Mech. **139**, 93–102 (2006).
[29] M. Pourjafar, H. Hamedi, and K. Sadeghy, "Stability of power-law fluids in creeping plane poiseuille: Effect of wall compliance," J. Non-Newtonian Fluid Mech. **216**, 22–30 (2015).
[30] M. Pourjafar and K. Sadeghy, "Linear stability of shear-thinning fluids in deformable channels: Effect of inertial terms," J. Non-Newtonian Fluid Mech. **230**, 80–91 (2016).
[31] Gaurav and V. Shankar, "Stability of pressure-driven flow in a deformable neo-Hookean channel," J. Fluid Mech. **659**, 318–350 (2010).
[32] P. Chokshi and V. Kumaran, "Weakly nonlinear analysis of viscous instability in flow past a neo-Hookean surface," Phys. Rev. E **77**, 056303 (2008).
[33] V. Gkanis and S. Kumar, "Instability of creeping Couette flow past a neo-Hookean solid," Phys. Fluids **15**, 2864–2471 (2003).
[34] C. Macosko, *Rheology: Principles, Measurements, and Applications* (VCH, New York, 1994).
[35] J. A. Weideman and S. C. Reddy, "A MATLAB differentiation matrix suite," ACM Trans. Math. Software **26**, 465–519 (2000).
[36] P. Drazin, *Introduction to Hydrodynamic Stability* (Cambridge University Press, Cambridge, 2002).
[37] P. J. Schmid and D. S. Henningson, *Stability and Transition in Shear Flows* (Springer, New York, 2001).